M. Dekker et al / Hacettepe J. Biol. & Chem., 2025, 53 (3), 57-69

Research Article

Hacettepe Journal of Biology and Chemistry

journal homepage: https://hjbc.hacettepe.edu.tr/
Dergipark Akademik: https://dergipark.org.tr/en/pub/hjbc

# Surface Pattern-Embedded Microfluidic Chip For Long-Term Maintenance of Hepatocytes

# Hücre Kültürlerinde Hepatosit Fonksiyonunun Uzun Süreli Korunumu için Yüzey Deseni İçeren Mikroakışkan Çip

**Minne Dekker[1], Anne-Marie Zeeman[2], and Burcu Gumuscu[1*]**

[1]Biosensors and Devices Lab, Biomedical Engineering Department, Eindhoven University of Technology, Eindhoven, 5612 AP, The Netherlands.
[2]Biomedical Primate Research Center, Rijswijk, 2288 GJ, The Netherlands.

## ABSTRACT

Functional hepatocytes are essential for drug screening and cytotoxicity studies, but primary hepatocytes lose their specialized functions within hours to days after seeding, limiting in vitro models for long-term assessments. To address this, we developed a microfluidic system that sustains long-term hepatocyte culture by optimizing flow conditions and incorporating microtopography to maintain cell-specific functions. A microfluidic chip with integrated topography was fabricated via soft lithography and characterized numerically. Flow parameters were optimized using HepaRG cells, and hepatocyte-specific functions were evaluated under static and flow conditions through albumin and urea assays. The system supported HepaRG cells for 25 days and primary macaque hepatocytes for 5 days. Flow conditions significantly enhanced metabolic activity, with HepaRG cells showing a 70-fold increase in albumin secretion and 40% higher urea production by day 14, and macaque hepatocytes exhibiting a 120-fold increase in albumin secretion by day 5 compared to static conditions. This optimized microfluidic platform offers a robust tool for drug screening and toxicity testing.

**Key Words**
Surface patterns, shear stress, organ-on-chip, hepatocytes, long-term cell culture.

## ÖZ

İşlevsel hepatositler, ilaç taraması ve sitotoksisite çalışmaları için önemlidir; ancak primer hepatositler, ekimden sonraki saatler veya günler içinde işlevlerini kaybeder, bu da in vitro modellerin uzun vadeli değerlendirmelerde kullanımını sınırlar. Bu sorunu çözmek için, hücreye özgü işlevleri korumak amacıyla akış koşullarını optimize eden ve mikro topografya içeren uzun vadeli hepatosit kültürünü destekleyen bir mikroakışkan sistem geliştirdik. Entegre topografyaya sahip bir mikroakışkan çip, litografi ile üretildi ve sayısal olarak karakterize edildi. Akış parametreleri HepaRG hücreleri kullanılarak optimize edildi ve hepatositlere özgü işlevler, albümin ve üre testleriyle statik ve akış koşulları altında değerlendirildi. Sistem, HepaRG hücrelerini 25 gün, primer makak hepatositlerini ise 5 gün boyunca destekledi. Akış koşulları, metabolik aktiviteyi önemli ölçüde artırdı; HepaRG hücreleri, statik koşullara kıyasla 14. günde albümin salgısında 70 kat artış ve üre üretiminde %40 daha yüksek bir artış gösterdi. Makak hepatositleri ise 5. günde albümin salgısında 120 kat artış sergiledi. Bu optimize edilmiş mikroakışkan platform, ilaç taraması ve toksisite testleri için uygun bir araç sunmaktadır.

**Anahtar Kelimeler**
Yüzey desenleri, kayma gerilimi, organ-on-chip, hepatositler, uzun süreli hücre kültürü.

**Article History:** Dec 24, 2024; Accepted: May 29, 2025; Available Online: Jun 30, 2025.
**DOI:** https://doi.org/10.15671/hjbc.1597749
**Correspondence to:** FB. Gumuscu, Biosensors and Devices Lab, Biomedical Engineering Department, Eindhoven University of Technology, Eindhoven, 5612 AP, The Netherlands.
**E-Mail:** b.gumuscu@tue.nl, burcugumuscu@gmail.com

## INTRODUCTION

The liver plays a pivotal role in metabolism, detoxification, and homeostasis, making it a primary focus for drug development and disease modeling. Traditional 2D cultures pawed the way to greatly improve our understanding of the liver cell function. To bring our understanding to a new level, there is a remaining need for better replicating the complexity of the liver microenvironment, leading to rapid dedifferentiation and functional loss [1,2]. While animal models provide closer physiological relevance, species differences and ethical concerns limit their utility [3,4]. Recent advances in microfluidics and surface engineering have demonstrated potential to overcome these challenges, allowing dynamic and structural cues to maintain hepatocyte viability and function over extended periods [5,6]. Particularly, long-term studies emphasize the importance of integrating multiple cues to improve the physiological relevance of hepatocyte cultures. Spheroid-based models extend hepatocyte functionality but lack perfusion and consistent access to nutrients [7,8].

Microfluidic liver-on-a-chip systems have been particularly effective in mimicking the liver's microenvironment, leveraging controlled flow to recreate physiological shear stress and nutrient gradients [9,10]. Devices incorporating microfluidic designs have successfully sustained hepatocyte functions such as albumin secretion, urea production, and cytochrome P450 activity for several weeks, making them invaluable for drug testing and disease modeling [11-13]. However, many of these platforms do not incorporate additional structural or mechanical cues that could further stabilize hepatocyte phenotype.

Apart from microfluidic models, a major emerging tool has been the surface patterning technology, which can regulate cell morphology, polarity, and differentiation through mechanotransduction pathways [14-17]. For instance, micro- and nano-patterned surfaces have been shown to maintain hepatocyte-specific markers and metabolic activity by mimicking the extracellular matrix [18-20]. Surface designs, including grooves and micropillars, direct cellular alignment and promote improved cell-matrix interactions, resulting in enhanced functionality compared to flat surfaces [21,22]. Despite these advances, static surface-patterning approaches often lack dynamic environmental factors critical for replicating in vivo-like conditions. By combining microfluidic flow and surface patterning, our novel platform addresses these limitations, enabling the investigation of how mechanical and biochemical cues jointly influence hepatocyte dedifferentiation and metabolic performance.

This study introduces a hybrid liver-on-a-chip device integrating flow dynamics and engineered surface patterns to achieve sustained hepatocyte function. Through metabolic assays, including albumin secretion, urea synthesis, and P450 enzyme activity, we demonstrate the superiority of this system in maintaining long-term hepatocyte performance, providing a robust model for drug discovery and preclinical research.

## MATERIALS and METHODS

Fabrication of microfluidic device and surface patterns

The surface patterns were fabricated in the MicroFab Lab facility at the Eindhoven University of Technology. The surface patterns were structured in 100 µm-thick polystyrene sheets via hot-embossing. We used standard photolithography to transfer surface patterns from mylar photomask (CAD/Art Services, Portland, USA) to an SU-8 mold. To achieve this, a 10 µm-thick SU-8 2010 layer was spincoated on a cleaned silicon wafer. We applied manufacturer's sheet (MicroChem, Germany) for applying spin rate, UV exposure dose, pre- and post-baking temperature and time in order to generate the patterns. The SU-8 coated wafer was pre-baked at 65°C for 5 minutes, exposed at 125 mJ $cm^{-2}$ (dose of 20 $mW.cm^{-2}$), and post-baked at 95°C for 3.5 minutes. The structures were developed using MR-600 developer (MicroChem, Germany). Finally, the SU-8 structures were treated with Trichloro(1H,1H,2H,2H-perfluorooctyl) silane (Sigma, Cat.: 448931) overnight. Next, PDMS (Sylgard®184) was prepared using 10:1 (w/w) elastomere base and curing agent, respectively. After degassing, the mixture was poured on SU-8 template and cured overnight at 65°C. A 1.5 mL OrmoStamp solution (MicroChem, Germany) was sandwiched between the PDMS template and a Borofloat wafer, which was spin-coated at 3000 rpm for 30 s with OrmoPrime08 (MicroChem, Germany) and baked at 150°C for 15 min. No air bubbles were left in the OrmoStamp solution at this stage. After 20 min, the sandwiched solution was exposed to UV light at 365 nm at a dose of 1000 mJ $cm^{-1}$ and intensity of 20 mW $cm^{-2}$. PDMS template was peeled off, and the polymerized OrmoStamp was had baked at 130°C for 30 min. The final thickness of

the OrmoStamp was measured as 150 µm. To enhance the detachment of the polystyrene after hot embossing, the Ormomould was plasma treated (Emitech K1050X, Germany) and silanized overnight. The OrmoStamp was brought in contact with a polystyrene sheet and hot embossed (Specac, Atlas Manual Hydraulic Press, Netherlands). The polystyrene sheet was heated above the glass transition temperature to 140 °C. After 5 minutes a hydraulic pressure of 5 tonnes was applied. The temperature and pressure were kept constant for 10 minutes before lowering the temperature to 90 °C. The pressure was reduced after reaching 90 °C. The polystyrene sheet was peeled off from the OrmoMould and treated with oxygen plasma at 50 Watt for 30 seconds.

The microfluidic chips were also fabricated in the MicroFab Lab facility at the Eindhoven University of Technology. The microchips were made of PDMS and prepared using SU-8 templates, which were produced as described above. SU-8 2100 was used to structure the channels with 500 µm height. PDMS layer was fabricated using PDMS mixed in a 10:1 ratio of silicone elastomer and curing agent. After mixing and degassing, the PDMS was cast on a SU-8 master mold and cured in the oven at 65°C for 35 minutes. After 35 minutes, the partially-cured PDMS was cut using a blade and the inlets were punched. The three layers, glass, polystyrene and PDMS, were bonded to assemble the chip. Figures S1 and S2 show the assembly steps of the chip. The backside of the polystyrene was glued to the microscope slide with Norland Optical Adhesive 81 (NOA81, Norland Products, USA) and exposed to 300 $mJ.cm^{-2}$. The polystyrene placed on the glass layer was plasma treated at 500 Watt for 30 seconds to clean the surface. Punched PDMS containing the microchannels was stamped on a thin layer of uncured PDMS, that was spin coated at 3000 rpm with 800 rpm acceleration for 60 seconds and placed on the polystyrene. The top of the polystyrene contained the surface patterns with an area of 1.17 x 0.31 cm. The microchannel was placed on this area. After the assembly, the PDMS layer was fully cured at 65 °C overnight.

The dimensions of the microfluidic device were 10000 x 5000 µm (width x breadth). The height of the chip was measured 520 µm using DektakXT (Bruker, Netherlands). The total volume of the chip was approximately 28 µL. The chips used for the cell culture experiments were sterilized using 70% Ethanol and washed with Phosphate-buffered saline (PBS) and culture medium. The tubes (Masterex Tygon Microbore Tubing, Sweden, OD = 1.52 mm, ID = 0.51 mm) were autoclaved before the cell culture.

**Hepatocytes cell lines, seeding and culture**

For the optimization study, HepaRG cells (kindly provided by Hubrecht Institute, Utrecht) were cultured under static and flow conditions in the chip on surface patterns and at flat surfaces. The seeding density was optimized for maximum viability of the cells in the chips and was $2.7x10^4$ cells $cm^{-1}$. The cells were cultured in William's E Medium with glutamax (Gibco, 32551020, Netherlands) supplemented with 10% fetal bovine serum (FBS), 1% penicillin/streptomycin mix (Pen/Strep), 50 mM Hydrocortison Succinate (Sigma-Aldrich, H2270, Netherlands) and 5 g $mL^{-1}$ insulin (Sigma-Aldrich, I2643, Netherlands). For the urea assay and CyQuant assay experiments the cells were cultured in William's E Medium with no phenol red (Gibco, A1217601, Netherlands) with the same additives and 5 $g.mL^{-1}$ L-Glutamine. The medium was collected on days 3, 8, 14, 20, 25, and 30 for static conditions and only on day 8 and 14 for flow conditions for the analyses of albumin and urea concentrations. The collected medium samples were stored at -20 °C until further analysis. For the CyQuant assay, the cells were trypsinized and the cell pellet was stored at 80 °C for a maximum of 28 days. The cells were fixed on day 4 under static and flow conditions on a flat surface and on day 8 under static condition on surface patterns. The volume of the static chip was enlarged with 200 µL pipette tips in the inlets and outlets, functioning as medium reservoirs. The medium was refreshed every two to three days. The volumetric flow in the flow conditions was 500 µL $h^{-1}$. The volumetric flow was applied using a syringe pump (Harvard Aparatus, PHD Ultra syringe pump, Germany) that was extended with a rack to place 10 syringes simultaneously. The cells were seeded in the chips under static condition via the inlet of the chip using a pipette, also for the flow conditions, the cells were attached to the pump after 24 hours under static conditions.

For the proof-of-concept study, cryopreserved primary macaque hepatocytes (PMH) (kindly provided by Hubrecht Institute, Utrecht) were cultured under static and flow conditions in the chip on surface patterns and at surfaces. After thawing, the cells were suspended in William's B Medium: William's E medium (Invitrogen, 32551-087, Netherlands) with 10% Human Serum A+, pooled, heat inactivated (Sanquin, the Netherlands), 1%

100X Pen/strep (Invitrogen, 15140-122, Netherlands), 1% 100X Insulin/-transferin/selenium supplement (Invitrogen, 41400-045, Netherlands), 1% 100 mM sodium pyruvate (Invitrogen, 11360-036, Netherlands), 1% 100X MEM-NEAA (Invitrogen 11140-035, Netherlands), 0.1 M hydrocortisone (Sigma, H0888, Netherlands) and 0.1% 2-mercaptoethanol (Invitrogen, 31350-010, Netherlands). The cells were washed with a 36% Percoll gradient to remove the dead cells. The cells were seeded at $2.1x10^5$ cells $cm^{-1}$ in William's B medium. The medium was changed to William's D medium (William's B medium plus 2% DMSO, Sigma, P1860, Netherlands) after 24 hours of incubation at 37°C, 5% $CO_2$.

The PMH are seeded on collagen coated surfaces in standard culture conditions. For this reason, the PMH were seeded in collagen coated commercially available 96 well-plates (Perkin Elmer, 96 well Cell Carrier Ultra, 60055700, USA), following the standard protocol. To observe the cell behavior on the surface patterns and at surfaces, the cells were seeded on the surface patterns and at surfaces in a 24 well-plate with and without a collagen coating. Finally, the cells were seeded in the microfluidic chip on the surface patterns and flat surface with a collagen coat. The surfaces were coated with a collagen solution of 5 mg $mL^{-1}$ collagen (Rat tail collagen type 1, Advanced Biomatrix 4mg $mL^{-1}$, 5056, USA) in 0.02M acetic acid in MilliQ water. Depending on the area, 5 $\mu g.cm^{-2}$ was applied.

**Functional assessment of hepatocyte metabolism**

We evaluated hepatocyte function via viability, albumin and urea assays, fluorescence staining, and morphological analysis. To monitor the cell viability and attachment of the cells in the chips under static and flow conditions, EVOS™ XL Core Imaging System (Netherlands) was used.

Human albumin ELISA (Thermo Fisher, EHALB, Netherlands) was used to quantify the concentration of albumin secreted by the cells. The albumin ELISA assay was performed according to the manufacturer's protocol. The samples were collected from the medium reservoir pipette tips (static condition) and for two hours (flow condition). A standard dilution series was prepared for every ELISA assay ranging from 1200 ng $mL^{-1}$ to 4.915 ng $mL^{-1}$. The sample dilution was determined by running the ELISA assay with a dilution series of the sample (2x, 10x, 20x, 40x and 100x) and 100x diluted samples were used for the measurements. The absorbance was read at 450 nm within 30 minutes after adding the stop solution with the plate reader (BioSPX, BioTek Synergy HTX).

The concentration of urea in the collected medium samples was quantified using a colorimetric urea assay (Bioassaysys, DIUR-100, Netherlands). To prevent interference, the assay was performed with cells cultured in medium with no phenol red. For the assay, 50 µL sample, 50 µL of urea 5 $mg.dL^{-1}$ and 50 µL water (blank) in duplicates were transferred into different wells. 200 µL working reagent was added to the wells and incubated for 50 minutes at room temperature. The optical density was read at 430 nm with the plate reader (BioSPX, BioTek Synergy HTX).

We quantified the cell number for the normalization of albumin and urea assays using a CyQuant kit (Thermo Fisher, C7026, Netherlands). The cells were seeded in medium containing no phenol red to prevent interference in the measurements. The cells were washed two times with PBS and incubated with 28 µL trypsin for 10 minutes. After the first incubation, an empty 200 µL pipette tip was placed in the outlet, and afterwards 200 µL was pushed into the chip via the inlet with a pipette. The medium was caught in the empty pipette tip. The medium was pushed back and forth with the pipette at least 10 times to detach all cells. The cell suspension was centrifuged for 5 minutes at 1500 rpm in a microcentrifuge. The cell pellets were kept at -80 °C for at least 12h. After thawing the pellet 200 µL CyQUANT GR dye/cell-lysis buffer was added, and the fluorescence was measured at 480 nm excitation and 520 nm emission maximum with the plate reader.

Fluorescence images were made to further characterize cell behavior on the chip. The HepaRG cells were washed with PBS and fixed in 3.7% Formaldehyde in PBS for 20 minutes at room temperature. The cells were permeabilized with PBS-Triton X-100 0.5% for 10 minutes at room temperature. The HepaRG cells were stained with Phalloidin (1:250) and Dapi (1:500) for 25 minutes. After all steps, the cells were washed three times with PBS. Images were captured using the Zeiss Axio Observer 7-Apotome (Germany).

The PMH the cells were fixed in 4% Paraformaldehyde in PBS for 30 minutes. The cells were stained for Phalloidin, Dapi. After washing the cells with PBS, the cells were incubated with the primary antibody (1:50) diluted in dilution buffer (0.15 g Triton X-100 and 0.5 g BSA in 50 ml PBS) at 4 °C overnight (approximately 20 hours)

and washed with PBS. Then the cells were incubated with the secondary antibody (Goat anti-Rabbit AF568, Invitrogen, A-11011) (1:1000), Phalloidin (1:400) and Dapi (1:500) at room temperature for 1.5 hours. The samples that were only stained for Phalloidin and Dapi were permeabilized with PBS-Triton X-100 0.5% for 10 minutes at room temperature and washed two times for 5 minutes with PBS and then stained with Phalloidin (1:400) and Dapi (1:500) for 1.5 hours. The cells on the polystyrene surfaces and in the chips were mounted. The chip samples were mounted by removing the PDMS microchannel and mounting a glass cover slide with Mowiol on top of the cells. The cells were imaged through the cover slide, so the sample was placed upside down in the microscope. The volumes used to stain the cells in the chips were adjusted to the maximum volume of the chip (28 µL). The chips were washed by slowly rinsing the chip three times with 1 mL PBS.

**Quantification of cell viability**

The viability assay was performed to determine the viability of the cells in the chips under static and flow conditions on day 5 after seeding. The cells seeded in a 24 well-plate were used as the control group. The cells were stained with Dapi and Propidium iodide (Molecular Probes, P3566) (PI). 1 mM reagents in DMSO solution of both stains were diluted in warm sterile medium with 1:100 ratio and added to the cell culture. The cells were incubated for 30 minutes at 37°C, 5% $CO_2$. Afterwards, the cells were incubated with a solution of PI in warm medium (1:100) for 20 minutes. The cells were washed three times with PBS after each staining step.

**Simulation of shear stress and fluidic conditions in microfluidic device**

The design is a simple chamber with one inlet and one outlet. The cell culture chamber of the chip is 1.5 cm (length) x 0.5 cm (width) x 500 µm (height). COMSOL Multiphysics software is used for simulating the flow and shear conditions in the chip with a volumetric flow of 500 $\mu L.h^{-1}$, where creeping flow, laminar flow and transport of diluted species modules were used in simulations. In the creeping flow module, we applied steady flow, incompressibility, negligible inertial forces and shallow channel approximation conditions. For the laminar flow, we applied steady flow, incompressibility, and a shallow channel approximation [23].

**Statistical analysis**

Statistical analysis was performed with Jamovi (version 2.2.5). Two-way ANOVA test was performed for the image analysis where more than two conditions were compared. Shapiro-Wilk test and Q-Q plot were used to determine the normality of the data. Tukey's multiple comparison test specified the differences between the conditions. The significance threshold for all tests was $p < 0.05$. Unpaired t-test was performed to analyze two independent groups with equal variance.

## RESULTS and DISCUSSION

**Enabling long-term hepatocyte culture in the surface pattern-embedded microfluidic chip**

The relevance and predictive accuracy of an in vitro liver model largely depend on the choice of cell source. Primary hepatocytes are widely regarded as the gold standard for in vitro liver models due to their representative metabolic activity and comprehensive hepatic functionality. However, their functionality declines rapidly under conventional culture conditions [24].

To address this challenge, we developed a microfluidic system designed to sustain hepatocytes for long-term studies. This system features a dual-function design: it provides a physiologically relevant shear rate and modulates cell behavior using repetitive surface patterns. Under these optimized conditions, we successfully preserved hepatocyte functionality for 25 days. The microfluidic chip includes a culture chamber measuring 1.5 cm (length) × 0.5 cm (width) × 500 µm (height) (Figure 1A). Embedded within the cell-growth area at the bottom of the channel are surface patterns with a height of 10 µm (Figure 1A, 1B), which contribute to the maintenance of hepatic functionality by mimicking key aspects of the native microenvironment.

We fabricated repetitive surface patterns on a polystyrene substrate using an SU-8 mold (Figure S1). The seeding area of the chip measures approximately 1.5 by 0.5 cm, with the chips having rounded edges. The surface patterns were arranged in a rectangular pattern measuring 1.17 by 0.31 cm to fit within the microfluidic chip, leaving a small border for attaching the polystyrene sheet to the polydimethylsiloxane (PDMS) culture chamber (Figure 1A). The quality and shape of the surface patterns were assessed using SEM and DektakXT. The surface pattern used in this study was selected because it has been shown to delay the de-differentiation

of primary human hepatocytes [25,26]. Figure 1A illustrates the PDMS stamp created from the SU-8 mold. The final surface pattern was imprinted onto polystyrene sheets (Figure S2). Edge sharpness and finer structural details were partially transferred during lithography and Ormocomp molding processes. Nevertheless, the imprinted structures maintained sufficient spacing between features to trap and confine cells, preserving their round morphology Figure 1B). The final measured height of the surface patterns was 8 µm.

Next, we fabricated and characterized microfluidic chips. To achieve various shear stress conditions in the microfluidic chips, an SU-8 master mold with 520 µm height was fabricated. This height provided the optimal balance of minimal shear stress and maximum nutrient perfusion, which are critical for sustaining cell viability and functionality. Hepatocytes are highly sensitive to shear stress exceeding 0.03 Pa [27], although low shear rates are beneficial for maintaining hepatic functions[28,29]. To support hepatocyte functionality, we applied low shear stress by directly flowing the culture media over the cells.

To optimize the conditions, we simulated the flow velocity, shear rate, and shear stress in the microfluidic channel using the following equations:

$$v=Q/A,\ \gamma=v/x$$
$$\tau=\gamma^{*}\mu$$

where $v$ is the flow velocity, $Q$ is the volumetric flow rate; $A$ is the cross-sectional area of material with area parallel to the applied force vector, γ is the shear rate, τ is the shear stress and µ is the dynamic viscosity of the flow. Given the inlet area of 2.78 x $10^{-4}$ $m^2$, we calculated the inlet velocity as 5.0 x $10^{-7}$ $m.s^{-1}$. Based on this input, the numerical studies (Figure 1C) confirmed a homogeneous, laminar flow within the microfluidic chip, with no turbulence or backflow. The shear stress profile, as expected, exhibited a downward parabolic shape due to friction between the fluid and the channel walls caused by the no-slip boundary condition. The maximum shear stress was calculated to be 1 x $10^{-4}$ Pa, which is 300 fold lower than the threshold shear stress that hepatocytes can physiologically tolerate [27]. To

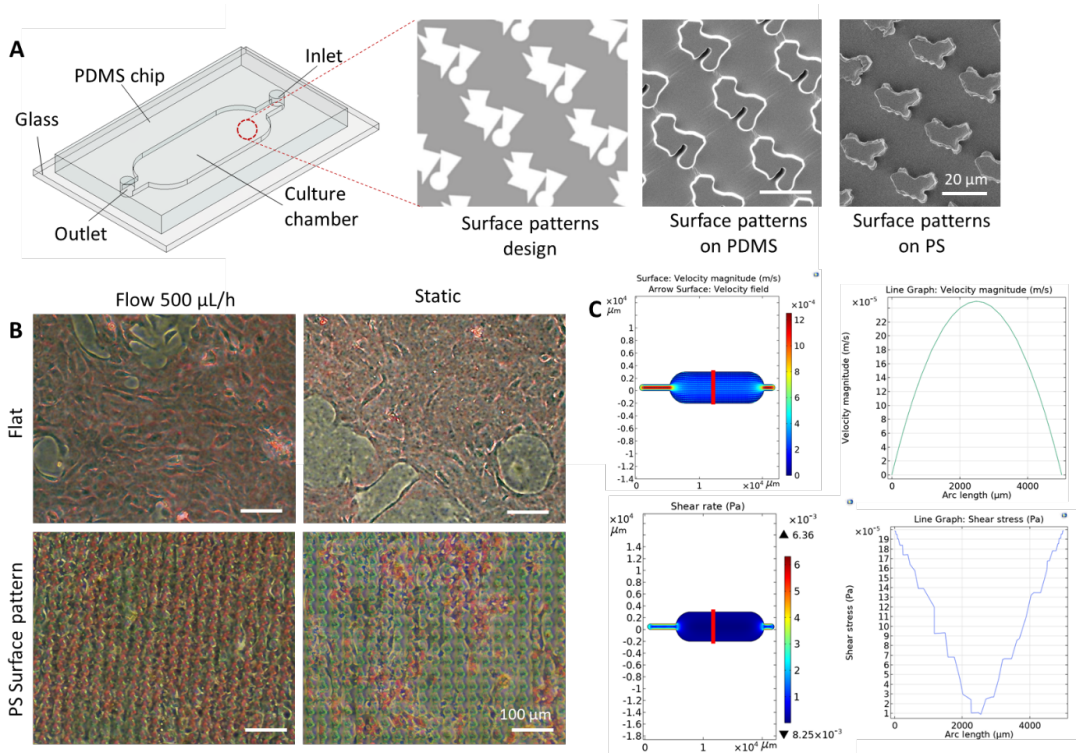


**Figure 1.** The long-term liver on chip. (A) The schematic view of the microfluidic chip containing the cell culture chamber, inlet and outlet. The cell culture chamber consists of polystyrene surface patterns that were fabricated by transferring the designed patterns onto an SU-8 mold, PDMS, and polystyrene material, accordingly. (B) The cultured hepatocytes under static and fluidic conditions on flat and patterned surfaces. The hepatocytes were artificially colored red and the surfaces were colored green for the ease of observation. (C) Numerical modeling of the flow rate (top) and shear stress (bottom) in the cell culture chamber. The red line indicates the local profiles of these parameters.

experimentally confirm the numerical results and to visualize the flow direction and speed, the chip was perfused with PBS solution containing 2 µm diameter fluorescent beads emitting a FITC signal. The imaged area was 903 × 903 µm, with a frame interval of 30 ms. The 200 µm-high chips were perfused at a flow rate of 1000 µL/h. The calculated flow velocity in the center of the chip was 2.78 x $10^{-4}$ m.$s^{-1}$, which closely matched the numerically characterized value of 2.5 x $10^{-4}$ m.$s^{-1}$.

We integrated the polystyrene-made repetitive surface patterns into PDMS chip as the next step. We started the assembly by bonding the underside of the polystyrene surface to a microscope slide using Norland Optical Adhesive 81 (NOA81). This biocompatible, transparent adhesive forms a hard polymer when exposed to UV light. To incorporate the surface patterns on the top side of the polystyrene into the microfluidic chip, PDMS cell culture chamber needed to be bonded to the polystyrene sheet. However, due to PDMS's low surface energy, this bonding process required a multi step procedure. First, the surfaces of both materials were treated with oxygen plasma, which cleaned and activated the surfaces by generating highly reactive oxygen radicals, reacting with organic molecules on the surface to create silanol groups. This process increased the wettability and hydrophilicity of the materials, facilitating adhesion. Next, we used a thin layer of uncured PDMS as the bonding medium. The uncured PDMS was spin-coated onto a glass slide at 3000 rpm to assemble a uniform layer. The PDMS chambers were then stamped into this uncured PDMS layer before attaching them to the polystyrene. To strengthen the bond, PDMS was partially cured by placing it at 65°C for 35 minutes. Finally, the partially cured PDMS was cut into rectangles and punched with a 2 mm diameter punch, slightly larger (by 0.49 mm) than the outer diameter of the tubes (1.51 mm) to account for the hourglass-shaped punched holes. The punched PDMS was subsequently stamped into the uncured PDMS and bonded to the polystyrene sheet. This method proved successful to assemble the microfluidic chip for flow condition experiments without leakage problems.

**Optimization of the surface pattern-embedded microfluidic chip for long-term experiments using HepaRG cells**

We optimized the static and fluidic cell seeding conditions using HepaRG cells. The seeding density was selected to be 2.6 x $10^{4}$ cells.$cm^{-2}$ in line with the recommended seeding density by the supplier [30]. Cell viability was quantified using CellProfiler, analyzing six images taken randomly from each sample per condition. HepaRG cells cultured in a well-plate served as positive control. The negative control consisted of cells incubated with 50% DMSO for 2 hours prior to staining. Results showed that cell viability in both the positive control and the chip under fluidic conditions exceeded 95%, while viability in the negative control was below 5% (Figure S3). These findings confirmed that the optimized flow conditions supported cell survival within the microfluidic chips [25,26].

The chips under static conditions confirmed the biocompatibility of the microfluidic platform, aligning with previous studies that demonstrated improved hepatocyte viability when exposed to flow conditions [31,32]. We thus hypothesized that introducing a low perfusion rate of 50 µL.$h^{-1}$ would enhance cell viability while retaining the function. Accordingly, the chips were connected to the pump 6 hours after seeding, as cell attachment occurred within this time frame in our preliminary experiments. The cells were initially exposed to a flow rate of 50 µL.$h^{-1}$, which corresponded to a shear stress of 4 x $10^{-4}$ Pa and flow velocity of 5.5 x $10^{-6}$ m.$s^{-1}$ in the center of the channel. At this rate, the medium in the chip was refreshed approximately 0.08 times per minute. For comparison, control groups were cultured under static conditions. The morphology of HepaRG cells under static conditions was comparable to cells cultured in previous well-plate experiments on day 3 (Figure 2A).

Under static conditions, cells formed a continuous monolayer (Figure S4A, S4B) and reached confluency by day 20 on flat surfaces, with cells showing a cuboidal, biliary-like morphology. Cells on surface patterns reached confluency by day 25, but most retained a cuboidal morphology, and hepatocyte islands were not clearly distinguishable (Figure 2). In fluorescent images of the static condition, the cells on flat surfaces had larger, round nuclei, some of which were marked by cortical actin, and appeared more tightly packed compared to those on the surface patterns (Figure S4A). Cells on surface patterns were deformed by the structures and had smaller, brighter nuclei, possibly indicating higher metabolic activity, as brighter nuclei can suggest less condensed chromatin and active transcription [33,34]. However, differentiation phenotypes were not clearly visible on surface patterns, and hepatocyte islands for-

med more slowly compared to flat surfaces.

In contrast, perfused cells reached full confluency by day 8 on both flat surfaces and surface patterns under fluidic conditions. The bright-field images (Figure 2, Figure S4) showed that structures resembling hepatocyte islands appeared on day 8 but disappeared by day 14. Morphology under fluidic conditions differed from static conditions: elongated cells began aligning by day 8, while smaller cuboidal cells appeared in other areas, suggesting cellular adaptation to the fluidic environment. By day 14, the alignment of cells perpendicular to the flow direction was more evident. Fluorescent imaging under fluidic conditions revealed that the cells were more elongated and separated, with longer actin fibers. The nuclei were significantly ($p = 0.0001$, $n = 1000$) larger and more elongated than those under static conditions, with a higher eccentricity value, indicating more elongated shapes. The alignment of nuclei and cells in the direction of flow, starting from day 8, was consistent with the morphological changes observed in the bright-field images (Figure 2, Figure S4).

Further analysis showed that the cells under fluidic conditions adapted to the surface patterns differently. Cells on the flat surfaces were more cuboidal with large round nuclei, while cells on the surface patterns were deformed by the structures and had smaller nuclei (Figure S4). In denser areas of the surface patterns, the cells rested more on top of the structures, while in less dense areas, the cells appeared more spread out. Interestingly, the nuclei of the cells on the surface patterns were brighter than those on flat surfaces, suggesting that these cells might have a higher metabolic activity. The intensity of Dapi staining, which is higher in less condensed chromatin [33,34], further supports this hypothesis. These findings suggest that HepaRG cells exhibit distinct morphological adaptations depending on the culture conditions, with flow conditions promoting alignment and elongation of cells and surface patterns influencing nuclear morphology and possibly metabolic activity. We observed slower differentiation in on-chip experiments under both static and fluidic conditions compared to well-plate experiments, yet the results demonstrate the suitability of the platform for long-term HepaRG culture.

To assess the metabolic function of HepaRG cells under static and fluidic conditions, medium samples were collected to quantify albumin and urea production. Static conditions and well-plate experiments served as controls. Waste medium was collected to quantify albumin and urea production by the HepaRG cells under both static and fluidic conditions. We hypothesized that fluidic conditions would enhance the metabolic functionality of the HepaRG cells. Albumin secretion was normalized for dilution, cell number, and sample collection duration, while urea concentration was normalized for cell number and collection duration to allow comparison with well-plate experiments. For comparing static

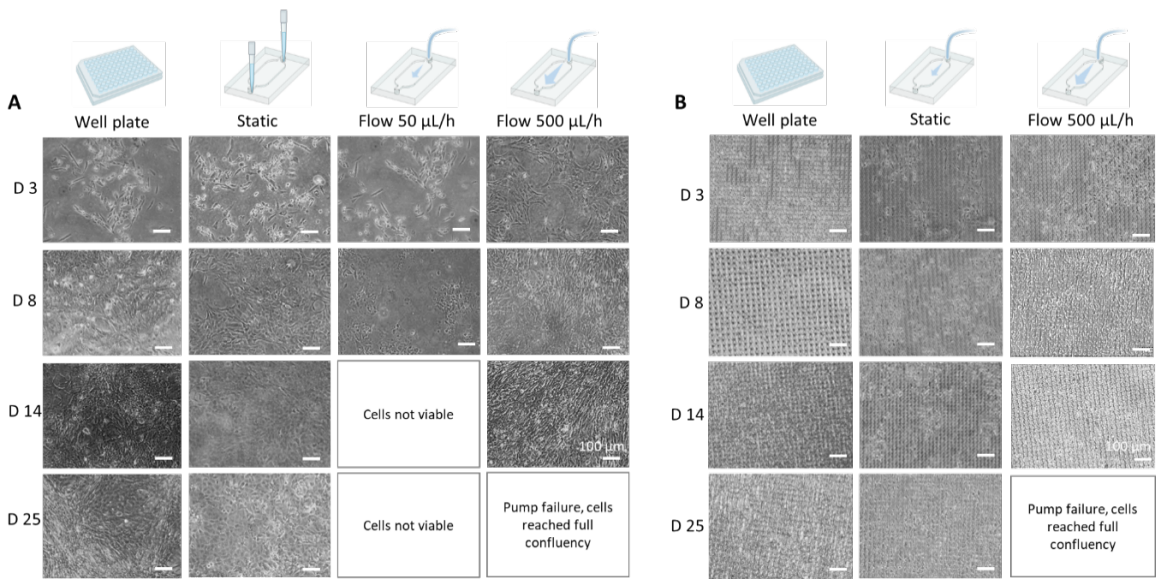


**Figure 2.** Bright field images of the HepaRG cells cultured in well-plate, static chips, and chips under fluidic conditions. (A) Long-term hepatocyte cell culture on flat surfaces, (B) long-term hepatocyte culture on patterned surfaces. The scale bar is 100 µm in all images. Letter D denotes the duration of the experiment in days.

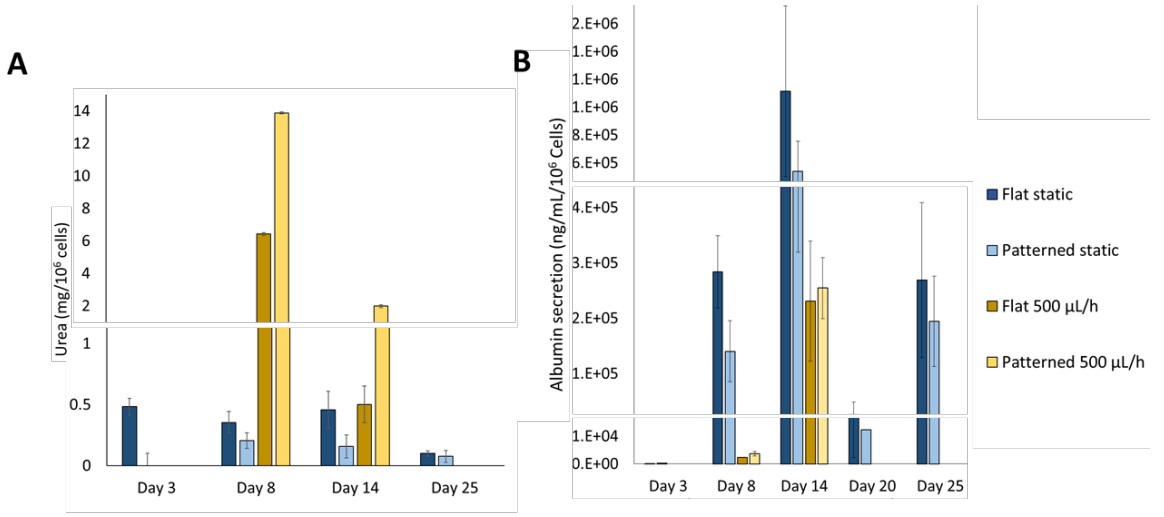


Table 1

**Figure 3.** The concentration of (A) albumin and (B) urea produced by HepaRG cells over time, cultured on surface patterns or flat surface under fluidic and static conditions.

and fluidic conditions, concentration values were also normalized to sample collection time.

Albumin secretion under static conditions, measured on days 8, 14, 20, 25, and 30 (Figure 3A), followed a similar trend to well-plate experiments, as expected [25,26]. Albumin secretion increased until day 14 and then dropped on day 20, corresponding to the transition of HepaRG cells from the proliferation phase to the differentiation phase. Lubberstedt et al. found that albumin secretion in HepaRG cells peaked at day 7 and remained stable through day 14 at an average rate of 3.3 $\mu g.day^{-1}$ $10^{-6}$ cells [35]. On day 14, albumin secretion in the static chip was 70 times higher than that reported by Lubberstedt et al. and 300 times higher than in the well-plate experiments. This discrepancy is likely due to the higher oxygen supply in the gas-permeable PDMS chips compared to the limited oxygen environment in the polystyrene well-plates, which may improve the metabolic function of hepatocytes [36].

The urea production by the HepaRG cells under static conditions decreased after day 14, following a similar pattern to the well-plate experiments, as the cells entered the differentiation phase (Figure 3B). The difference between flat surfaces and surface patterns was more pronounced during the first 14 days, though the variability was high (Figure 3B). Urea production was comparable to levels observed in previous well-plate experiments [25,26]. Lubberstedt et al. did not observe urea production in HepaRG cells treated with 2% DMSO, which is known to induce differentiation and enhance drug-metabolizing functions, yet suppresses functions like urea production [35,37].

Albumin secretion under fluidic condition followed a similar trend as the static condition but was 120 times lower on day 8, with comparable levels on day 14 (Figure 3A). Urea production under fluidic conditions was notably higher on day 8, and similar to static conditions on day 14. Interestingly, urea production was higher on the surface patterns under fluidic conditions (Figure 3B). Other studies have reported higher albumin and urea production under fluidic conditions, i.e., 4.8$mg.h^{-1}$ $10^{-6}$ cells on day 9 and 1.8 $mg.h^{-1}.10^{-6}$ cells on day 13) [38]. However, higher shear stress (0.5 to 2.1 Pa) can reduce both albumin and urea production [32].

**Expanding primary hepatocyte culture in the surface pattern-embedded microfluidic chip for enhanced liver functionality**

Primary hepatocytes undergo dedifferentiation within days of in vitro culture, resulting in changes in morphology and a reduction in hepatic function which differs from HepaRG cells. We hypothesized that primary macaque hepatocytes (PMH) would survive in the optimized microfluidic chip for at least 5 days and that the combination of surface patterns and fluidic conditions would support their function by alleviating mechanical

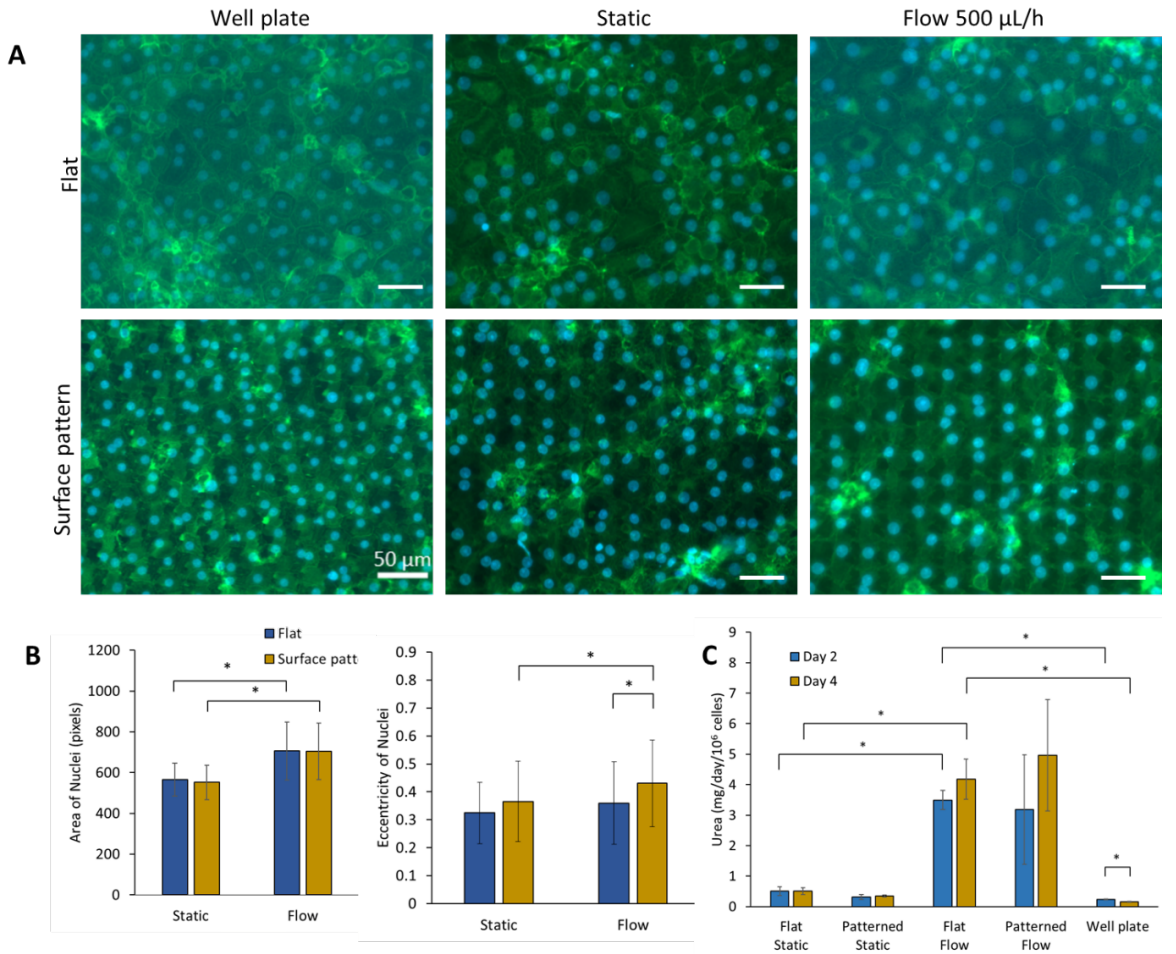


**Figure 4.** The PMH cell response to on-chip experiments. (A) PMHs in well-plates as well as on flat and patterned surfaces under static and fluidic conditions. The nuclei are stained in blue, and actin is stained in green. Images were captured using a 20x objective using the Zeiss Apotome Observer 7 microscope. The scale bar represents 50 µm in all images. Flow direction was horizontal. (B) Nuclei morphology analysis with CellProfiler focusing on area and eccentricity of nuclei on patterned and flat surfaces in the well-plate and on-chip on days 2 and 4, * indicates a significant difference ($p < 0.05$). (C) Urea secretion by PMH on patterned and flat surfaces under static and fluidic conditions on days 2 and 4. The control group consists of PMH cultured on collagen-coated well-plates. * indicates a significant difference ($p < 0.05$).

tension, while ensuring continuous nutrient supply and waste removal. Markers for assessing hepatocyte differentiation include cell morphology and urea synthesis as a functional indicator of the hepatic phenotype. The PMH were cultured on surface patterns and flat surfaces with a collagen coating, under both static and flow conditions. As a control, cells were seeded in commercially collagen-coated well-plates, as well as in regular well-plates with and without collagen on patterned and flat surfaces. The seeding density was $2 \times 10^5$ cells.cm$^{-2}$ in both well-plates and chips. When perfused, PMH were exposed to flow 24 hours post-seeding at a rate of 500 µL.h$^{-1}$, generating a shear stress of 6.4 x $10^{-4}$ Pa, comparable to the flow conditions used for HepaRG cells.

We initially determined the necessity of collagen coating by comparing cell attachment on surfaces with and without collagen. On collagen-coated flat surfaces, PMH morphology on days 2 and 4 resembled that of the control, which might have inconsistencies in the collagen coating. On surface patterns with collagen, PMH formed a continuous monolayer. The nuclei were positioned between the patterned structures, some deformed by the surface patterns, and all aligned in rows. Cytoplasm was visible on top of the structures, but the morphology of the cytoplasm and nuclei were unaffected by the surface patterns. The cells were more elevated on surface patterns on day 4 compared to day 2, with increased cortical actin observed (Figure S5). In

contrast, on surfaces without the collagen coating, cell attachment was notably lower, with small cell islands observed on the flat surface. As shown in Figure S5, the hexagonal shape was rarely visible, and cells exhibited an increased actin fiber presence. On surface patterns without collagen, cells did not form a continuous monolayer, but the morphology of the islands resembled that on surface patterns with collagen coating. We decided to use collagen coating according to these results.

During the chip seeding, fluorescent images were taken on days 2 and 4 to evaluate PMH morphology on surface patterns and flat surfaces under static and fluidic conditions, with the well-plate experiments serving as the control. In standard culture conditions, PMH began to dedifferentiate within hours, as evidenced by changes in cell morphology. On day 2, the PMH exhibited the characteristic hexagonal shape, with large cells, one or more round nuclei, and a monolayer that covered the surface, surrounded by cortical actin. Figure 4A shows that by day 4, the cell borders were less distinct, the cortical actin was less prominent, and the hexagonal shape became harder to discern, indicating dedifferentiation. In contrast, surface patterns were expected to confine the cells, prevent flattening, alleviate mechanical tension, and potentially inhibit dedifferentiation [39].

PMH were seeded in the chip under static and flow conditions to assess their morphology and viability, confirming the chip's optimization for primary hepatocytes. Under static conditions, cells on the flat surface formed clusters with increased actin fibers and some clusters with minimal actin. Only a few cells had defined borders by cortical actin. In contrast, cells on the flat surface under fluidic conditions displayed cortical actin and retained a hexagonal shape, similar to the control. On surface patterns in the microfluidic chip, the cells were elevated on patterned structures, with nuclei positioned between the structures and aligned in rows, while the cytoplasm covered the surface patterns more. Fluidic conditions caused the formation of smaller cell clusters with increased actin fibers and no cortical actin. Analysis of nuclei size, number, and eccentricity using CellProfiler revealed that on day 2, nuclei on the flat surface in the well-plate were significantly larger than those on surface patterns (Figure 4B). On day 4, nuclei on surface patterns were significantly larger than on day 2, with a notable increase in eccentricity, indicating more elongated nuclei on the patterned surfaces (Figure 4B). Under fluidic conditions, nuclei were significantly larger on day 4, and patterned surfaces produced more elongated nuclei compared to flat surfaces under both static and fluidic conditions. The results suggest that nuclear morphology is sensitive to both surface patterns and flow exposure.

Differentiated hepatocytes exhibit a cuboidal or hexagonal shape with enhanced cell borders and specialized structures like bile canaliculi [40,41]. Dedifferentiation is marked by cell flattening, weakened cell borders, and the loss of specialized structures, with cells sometimes adopting fibroblast-like shapes. The dedifferentiation of PMH is indicated by the formation of actin fibers and the loss of hexagonal shape. However, in our experiments, PMH formed a monolayer similar to the well-plate control, suggesting that the optimized flow conditions did not harm the cells. On flat surfaces, the morphology and hexagonal shape of PMH remained comparable to day 2 in the well-plate, with no additional morphological markers of dedifferentiation, indicating that the chip conditions support long-term culture.

The urea concentration was measured to assess the functionality of PMH under different culture conditions (Figure 4C). Medium samples were collected on days 2 and 4 from the collagen coated well-plate, regular well-plate, and the chips under both static and fluidic conditions. On both day 2 and day 4, urea production in the chips under fluidic conditions was significantly higher ($p < 0.05$, $n = 2$) on the flat surface compared to the static condition and the control. Additionally, PMH cultured in the chip under both static and fluidic conditions demonstrated increased urea production on day 4, whereas a significant decrease ($p = 0.0314$, $n = 2$) in urea synthesis was observed in the control on day 4.

In long-term cultures of primary hepatocytes, urea production typically declines over time as the cells undergo dedifferentiation [35,39,42]. However, the observed increase in urea production under fluidic conditions suggests that the flow may have helped maintaining differentiated hepatic functions of the PMH over four days. This observation aligns with findings by Jellali et al., who reported higher albumin and urea production in fluidic conditions [38]. These results support our hypothesis that fluidic conditions in the microfluidic chip help sustain hepatic function in PMH.

## Conclusion

We successfully developed and optimized a surface pattern-embedded microfluidic chip that supports long-term hepatocyte culture and enhances hepatic functionality under static and fluidic conditions. The chip sustained hepatocyte functionality for up to 25 days, with HepaRG cells demonstrating significantly higher albumin secretion (up to 300-fold) and urea production compared to conventional well-plate controls. Flow conditions promoted cell alignment, elongated nuclear morphology, and metabolic activity, with shear stress maintained at a physiological level of $4 \times 10^{-4}$ Pa. Similarly, primary macaque hepatocytes cultured in the chip under fluidic conditions showed a 2.5-fold increase in urea production by day 4 compared to static controls, highlighting the platform's ability to preserve differentiated hepatic functions. These findings confirm the chip's potential for long-term liver cell culture, offering a physiologically relevant system for drug metabolism and toxicity studies.

**Acknowledgement**

We thank all the Biosensors and Devices Lab and BioInterface Sciences Group members for helpful discussions and suggestions throughout the study. We thank Jan de Boer for his insightful contributions throughout the project and Joska Aerts for her contributions in the chip fabrication and off-chip experiments. This work was supported by the grant from TU/e Irene Curie Fellowship (to BG).

## References

1. P. Godoy, et al., Recent advances in 2D and 3D in vitro systems using primary hepatocytes, Hepatol. , 57 (2013) 550–559.
2. J. Wang, D. Huang, H. Yu, Y. Cheng, H. Ren, Y. Zhao, Developing tissue engineering strategies for liver regeneration." Eng. Regen., 3, (2022) 80-91.
3. M. R. Schneider, M. Oelgeschlaeger, T. Burgdorf, P. van Meer, P. Theunissen, A. S. Kienhuis, A. H. Piersma, R. J. Vandebriel, Applicability of organ-on-chip systems in toxicology and pharmacology, Crit. Rev. Toxicol., 51 (2021) 540-554.
4. G. Sipes, W. Bracken, M. Dorato, K. V. Deun, P. Smith, B. Berger, A. Heller, Concordance of toxicity of pharmaceuticals in humans and animals, Regul. Toxicol. Pharmacol., 32 (2000) 56–67.
5. K. H. Lee, J. Lee, S. H. Lee, 3D liver models on a microplatform: well-defined culture, engineering of liver tissue and liver-on-a-chip, Lab Chip 15 (2015) 3822-3837.
6. L. A. Vernetti, N. Senutovitch, R. Boltz, R. DeBiasio, T. Y. Shun, A. Gough, D. L. Taylor, A human liver microphysiology platform for investigating physiology, drug safety, and disease models, Exp. Biol. Med., 242 (2017) 1605–1619.
7. S. J. Fey, K. Wrzesinski, Determination of drug toxicity using 3D spheroids constructed from an immortal human hepatocyte cell line. Toxicol, Sci. 127 (2012) 403-411.
8. T. Kostrzewski, T. Cornforth, S. A. Snow, La. Ouro-Gnao, C. Rowe, E. M. Large, D. J. Hughes, Three-dimensional perfused human in vitro model of non-alcoholic fatty liver disease, World J. Gastroenterol., 23 (2017) 204.
9. A. Ehrlich, D. Duche, G. Ouedraogo, Y. Nahmias, Challenges and opportunities in the design of liver-on-chip microdevices. An. Rev. Biomed. Eng. 21 (2019) 219-239.
10. K. J. Jang, M.A. Otieno, J. Ronxhi, H.K. Lim, L. Ewart, K. R. Kodella, D. B. Petropolis, G. Kulkarni, J. E. Rubins, D. Conegliano, J. Nawroth, Reproducing human and cross-species drug toxicities using a liver-chip, Sci. Transl. Med., 11(517) (2019) eaax5516.
11. R. Baudoin, A. Corlu, L. Griscom, C. Legallais, E. Leclerc, Trends in the development of microfluidic cell biochips for in vitro hepatotoxicity, Toxicol. In Vitro 21 (2007) 535-544.
12. T. Messelmani, L. Morisseau, Y. Sakai, C. Legallais, A. Le Goff, E. Leclerc, R. Jellali, Liver organ-on-chip models for toxicity studies and risk assessment, Lab Chip 22 (2022) 2423-2450.
13. N. K. Inamdar, J. T. Borenstein, Microfluidic cell culture models for tissue engineering, Cur. Opin. Biotechnol., 22 (2011) 681-689.
14. Y. Du, N. Li, H. Yang, C. Luo, Y. Gong, C. Tong, Y. Gao, S. Lü, M. Long, Mimicking liver sinusoidal structures and functions using a 3D-configured microfluidic chip, Lab Chip 17 (2017) 782-794.
15. H. V. Unadkat, M. Hulsman, K. Cornelissen, B. J. Papenburg, R. K. Truckenmüller, A. E. Carpenter, M. Wessling, G. F. Post, M. Uetz, M.J. Reinders, D. Stamatialis, An algorithm-based topographical biomaterials library to instruct cell fate, Proc. Natl. Acad. Sci. U.S.A., 108 (2011) 16565–16570.
16. N. R. M. Beijer, A. S. Vasilevich, B. Pilavci, R. K. Truckenmüller, Y. Zhao, S. Singh, B. J. Papenburg, J. de Boer, TopoWellPlate: A well-plate-based screening platform to study cell–surface topography interactions, Adv. Biosyst., 1 (2017) 1700002.
17. N. R. Beijer, Z. M. Nauryzgaliyeva, E. M. Arteaga, L. Pieuchot, K. Anselme, J. van de Peppel, A. S. Vasilevich, N. Groen, N. Roumans, D. G. Hebels, J. de Boer, Dynamic adaptation of mesenchymal stem cell physiology upon exposure to surface micropatterns, Sci. Rep., 9 (2019) 45284.
18. J. You, V. K. Raghunathan, K. J. Son, D. Patel, A. Haque, C. J. Murphy, A. Revzin, Impact of nanotopography, heparin hydrogel microstructures, and encapsulated fibroblasts on phenotype of primary hepatocytes, ACS Appl. Mater. Int. 7 (2015) 12299-12308.
19. B. G. Munoz-Robles, I. Kopyeva, C. A. DeForest, Surface patterning of hydrogel biomaterials to probe and direct cell–matrix interactions, Adv. Mater. Int. 7 (2020) 2001198.
20. M. Ortega-Ribera, J. Yeste, R. Villa, J. Gracia-Sancho, Nanoengineered Biomaterials for the treatment of liver diseases, Nanoengineered biomaterials for regenerative medicine, Elsevier Press, New York, USA, 2019.
21. E. Zahmatkesh, A. Othman, B. Braun, R. Aspera, M. Ruoß, A. Piryaei, M. Vosough, A. Nüssler, In vitro modeling of liver fibrosis in 3D microtissues using scalable micropatterning system, Arch. Toxicol., 96 (2022) 1799-1813.
22. S.A. Abdellatef, A. Ohi, T. Nabatame, A. Taniguchi, The effect of physical and chemical cues on hepatocellular function and morphology, Int. J. Mol. Sci., 15 (2014)4299-4317.
23. C. Poon, Measuring the density and viscosity of culture media for optimized computational fluid dynamics analysis of in vitro devices, J. Mech. Behav. Biomed. Mater., 126 (2022) 105024.

24. V. Vilas-Boas, A. Cooreman, E. Gijbels, R. Van Campenhout, E. Gustafson, S. Ballet, P. Annaert, B. Cogliati, M. Vinken, Primary hepatocytes and their cultures for the testing of drug-induced liver injury, Adv. Pharmacol., 85 (2019) 1–30.
25. J. Aerts, Development of a microfluidic system for the long-term culture of hepatocytes, M.Sc. dissertation, Technol. Univ. Eindhoven, 2021.
26. M. Dekker, Assessment of the dynamic interplay of shear stress and surface topographies on hepatocytes in a microfluidic platform, M.Sc. dissertation, Technol. Univ. Eindhoven, 2022.
27. A. Bachmann, M. Moll, E. Gottwald, C. Nies, R. Zantl, H. Wagner, B. Burkhardt, J. J. M. Sánchez, R. Ladurner, W. Thasler, G. Damm, 3D cultivation techniques for primary human hepatocytes, Microarrays, 4 (2015) 64–83.
28. J. Park, F. Berthiaume, M. Toner, M.L. Yarmush, A.W.Tilles, Microfabricated grooved substrates as platforms for bioartificial liver reactors, Biotechnol. Bioeng., 90 (2005) 632–644.
29. Y. C. Toh, T. C. Lim, D. Tai, G. Xiao, D. van Noort, H. Yu, A microfluidic 3D hepatocyte chip for drug toxicity testing, Lab Chip, 9 (2009) 2026–2035.
30. HepaRG - Features [Online]. Available: https://www.heparg.com/rubrique-features (Accessed on 13 March 2025).
31. H. Rashidi, S. Alhaque, D. Szkolnicka, O. Flint, D. C. Hay, Fluid shear stress modulation of hepatocyte-like cell function, Arch. Toxicol., 90 (2016) 1757–1761.
32. A. W. Tilles, H. Baskaran, P. Roy, M. L. Yarmush, M. Toner, Effects of oxygenation and flow on the viability and function of rat hepatocytes cocultured in a microchannel flat-plate bioreactor, Biotechnol. Bioeng., 73(2001) 379–392.
33. G. Mascetti, S. Carrara, L. Vergani, Relationship between chromatin compactness and dye uptake for in situ chromatin stained with DAPI, Cytom.: J. Int. Soc. Anal. Cytol., 44 (2001) 113–119.
34. R. M. Martin, M. C. Cardoso, Chromatin condensation modulates access and binding of nuclear proteins, FASEB J., 24 (2010) 1066.
35. M. Lübberstedt, U. Müller-Vieira, M. Mayer, K. M. Biemel, F. Knöspel, D. Knobeloch, A. K. Nüssler, J. C. Gerlach, K. Zeilinger, HepaRG human hepatic cell line utility as a surrogate for primary human hepatocytes in drug metabolism assessment in vitro, J. Pharmacol. Toxicol. Methods, 63 (2011) 59–68.
36. S. Kidambi, R. S. Yarmush, E. Novik, P. Chao, M. L. Yarmush, Y. Nahmias, Oxygen-mediated enhancement of primary hepatocyte metabolism, functional polarization, gene expression, and drug clearance, Proc. Natl. Acad. Sci., 106 (2009) 15714–15719.
37. R. Hoekstra, G. A. A. Nibourg, T. V. van der Hoeven, M. T. Ackermans, T. B. M. Hakvoort, T. M. van Gulik, W. H. Lamers, R. P. Oude Elferink, R. A. F. M. Chamuleau, The HepaRG cell line is suitable for bioartificial liver application, Int. J. Biochem. Cell Biol., 43(2011) 1483–1489.
38. R. Jellali, T. Bricks, S. Jacques, M. J. Fleury, P. Paullier, F. Merlier, E. Leclerc, Long-term human primary hepatocyte cultures in a microfluidic liver biochip show maintenance of mRNA levels and higher drug metabolism compared with Petri cultures, Biopharm. Drug Dispos., 37 (2016) 264–275.
39. P. Sun, G. Zhang, X. Su, C. Jin, B. Yu, X. Yu, Z. Lv, H. Ma, M. Zhang, W. Wei, W. Li, Maintenance of primary hepatocyte functions in vitro by inhibiting mechanical tension-induced YAP activation, Cell Rep., 29 (2019) 3212–3222.
40. K. Meyer, H. Morales-Navarrete, S. Seifert, M. Wilsch-Braeuninger, U. Dahmen, E. M. Tanaka, L. Brusch, Y. Kalaidzidis, M. Zerial, Bile canaliculi remodeling activates YAP via the actin cytoskeleton during liver regeneration, Mol. Syst. Biol., 16 (2020) e8985.
41. M. Hegde, R. Jindal, A. Bhushan, S. S. Bale, W. J. McCarty, I. Golberg, O. B. Usta, M. L. Yarmush, Dynamic interplay of flow and collagen stabilizes primary hepatocytes culture in a microfluidic platform, Lab Chip, 14 (2014) 2033–2039.
42. J. Li, R. S. Settivari, M. J. LeBaron, M. S. Marty, Functional comparison of HepaRG cells and primary human hepatocytes in sandwich and spheroid culture as repeated-exposure models for hepatotoxicity, Appl. In Vitro Toxicol., 5 (2019) 187–195.